(1)

Observations of High Frequency and High Wavenumber Solar Oscillations

D. N. Fernandes, P. H. Scherrer
Center for Space Science and Astrophysics
Stanford University, Stanford, CA 94305, U.S.A.

T. D. Tarbell, A. M. Title
Lockheed Palo Alto Research Laboratories
O/91-30 B/256, 3251 Hanover Street, Palo Alto, CA 94304, U.S.A.

Accepted 1991 December 27
To appear in THE ASTROPHYSICAL JOURNAL
1992 June 20

Statement A per telecon
Dr. Neal Sheeley ONR/Code 1114
Arlington, VA 22217-5000

NWW 5/7/92

Abstract

Doppler shift measurements of the Na D_1 absorption line have revealed solar oscillations in a new regime of frequency and wavenumber. Oscillations of vertical velocities in the temperature minimum and low chromosphere of the Sun are observed with frequencies ranging up to 9.5 mHz. The *fundamental* modes appear with wavenumbers up to 5.33 Mm^{-1} (equivalent spherical harmonic degree, 3710). We find no evidence for chromospheric modes of 3 minute period.

Doppler shifts and intensities were measured for the core of the Na D_1 absorption line using the Orbiting Solar Laboratory evaluation, tunable-filter system, and CCD camera (Title *et al.* 1991) at the Swedish Solar Observatory. Filtered images (filtergrams) were taken at three wavelength offsets ($-85, 0, +80$ mÅ) from the nominal line center. The filter width was $\sim$ 62 mÅ (FWHM). Hence, the measurement was sensitive to line-of-sight velocities 500–900 km above the photosphere (Schleicher 1976).

Active region AR 6181 was observed for 2.4 hr on 1990 August 2 using the Swedish 50 cm vacuum solar telescope on La Palma, Spain. The 224" × 224" field of view was resolved into 512 × 512 pixels. A set of filtergrams was taken every 17.7 s for a total of 480 pairs of Doppler measurements (Dopplergrams) and intensity measurements. The angular size of the field of view was determined to within 1% by comparison of magnetograms from La Palma and from the National Solar Observatory at Kitt Peak.

Reduction of filtergrams included calibration for the CCD detector response and removal of image rotation and drift caused by the telescope tracking. The effect of atmospheric "seeing" was minimized by "de-stretching" (November 1986) to remove image distortion, and spatial filtering to normalize the modulation transfer function (MTF) of the atmosphere. The "MTF normalization" forces the spatial spectrum of each filtergram of a given wavelength to look like the average spectrum for filtergrams of that wavelength. Doppler shifts and line-center intensities were then calculated at each pixel by solving for the vertex of a parabola through the three filtergram intensities.

Three-dimensional Fourier transforms were made of the sets of Dopplergrams and intensities after apodization in the space and time directions. Both the full field of view and a 79" × 79" subfield of "quiet" Sun were transformed. The temporal and spatial Nyquist frequencies were 28.3 mHz and 9.9 Mm^{-1}, respectively. The distribution of power in Fourier $(\vec{k}, \nu)$ space as expected for acoustic waves (p-modes) and surface waves (f-modes) defines "trumpet"-shaped surfaces (Hill 1988) of approximate form $\nu \propto \|\vec{k}\|^{\frac{1}{2}}$.

Because the telescope was tracking the active region, there is no net motion of the medium across the field of view. Hence, the frequency of a "trumpet" at wavenumber $\vec{k}$ is the same as the frequency at $-\vec{k}$. The active region, however, was 17° from disk-center, causing waves propagating toward or away from disk center to appear at higher wavenumber than waves propagating in the perpendicular direction. This foreshortening distorts the cylindrical symmetry of the "trumpets" to give them an elliptical rather than circular cross section.

The power spectra were integrated in the azimuthal direction with allowance made for the foreshortening. The two-dimensional k-ν spectrum for the full-field Dopplergrams is shown in Figure 1. The p-mode and f-mode ridges are clearly visible at 5.5 mHz, but there is not a horizontal band of power near the "avoided crossings" as would be expected for a 3 minute chromospheric resonance (Ulrich & Rhodes 1977).

In addition to producing the power spectrum, the three-dimensional Fourier transform was used to study the phase of the oscillations. The phase difference between velocity and intensity oscillations was measured to be $\sim 0°$ for all visible ridges.

Slices of the power spectra were fitted using a nonlinear, weighted, least-squares fitting program. The weights were determined by the statistical error on the measured power, which in turn was derived from an assumed error of 50 m/s in the velocity measurement. The assumed power spectrum shape consisted of a power-law background, $P_k(\nu) = A_k \nu^{-B_k}$, together with Gaussian ridges.

The background parameters, A_k and B_k, were fitted independently for each wavenumber slice of each spectrum. The fit included a range of frequencies on either side of the ridges: $(0.12 < \nu/\mathrm{mHz} < 1.3)$ and $(12.0 < \nu/\mathrm{mHz} < 15.0)$. The background velocity power, integrated over frequency, is plotted in Figure 2. The spectrum falls off much more slowly with wavenumber than the spectrum of convection in the photosphere reported by Chou *et al.* (1991). We find a root mean square velocity of about 820 m/s for convection in the low chromosphere.

The ridges were fitted simultaneously after subtracting the background. Frequencies of ridges from the velocity spectra are plotted in Figure 3 with their respective statistical errors. All points plotted correspond to fits in which the offset, width, and height of the Gaussian converged to physically reasonable values, and the integrated power under the Gaussian was at least 4 standard deviations above the background.

The mode power is plotted as a function of frequency in Figure 4. Mode power is defined as the integral under the fitted Gaussian. The p-mode power has the same frequency dependence for all p-ridges. There is very little explicit wavenumber dependence. Power increases as $\nu^{7.3}$ to a maximum at 3.4 mHz, at which point it turns over and falls off again as $\nu^{-4.6}$. The f-modes have less power at a given frequency than the p-modes. As surface gravity waves with very little compression they are physically different from the p-modes and are not expected to show the same power spectrum.

An MTF correction was made to the power plotted in Figures 2 and 4 by combining the calculated MTF of the telescope and CCD with an estimated atmospheric MTF. The latter was derived from the difference between power spectra of the "MTF normalized" filtergrams and the sharpest filtergrams in the set. Since even the best images will still include some atmospheric blurring, this correction will provide an underestimate for power at the highest wavenumbers.

All six fitted p-mode ridges extend up to at least 7.0 mHz. The p_5 and p_6 ridges extend up to a frequency of 9.5 mHz. We see no deviation from a smooth extrapolation of the ridges at lower frequencies. This suggests that there are no new cavity resonances in the high frequency range revealed in this work. Libbrecht, Woodard & Kaufman (1990) have made measurements that overlap with ours at frequencies up to 5.3 mHz. The two data sets agree to within the experimental scatter of ± 15 μHz.

The f-ridge is visible at wavenumbers up to 5.33 Mm^{-1}. There is, however, a systematic discrepancy between frequencies fitted from the velocity and intensity spectra. Frequencies measured from the velocity spectra are consistently higher than those from the intensity spectra by up to 40 μHz at wavenumbers below 2.5 Mm^{-1}. This difference increases to $\sim$ 100 μHz at 4 Mm^{-1}. The discrepancy may in part be due to a difference between background shapes in the velocity and intensity spectra.

Libbrecht *et al.* (1990) report a Gaussian background, centered near 3 mHz, in their velocity spectrum. Inclusion of such a background in our fit would bring the f-ridge frequencies into better agreement at wavenumbers below 1.1 Mm^{-1}, but would push them farther apart at higher wavenumbers. Fitting such a background function, moreover, would require a longer time series with correspondingly better signal-to-noise ratio. It is noteworthy that the f-mode frequencies measured from the intensity spectra agree with those reported by Libbrecht *et al.* to within 15 μHz.

The discrepancy could also be caused by a difference in mode frequencies in the magnetic and nonmagnetic regions within the field of view. The weighting of magnetic regions is different for intensity and velocity spectra.

Regardless of which set of f-mode frequencies we use, the measured frequencies lie below the theoretical frequencies given by $\omega^2 = gk$ at wavenumbers greater than 1 Mm^{-1}. The difference is 100–200 μHz at 4 Mm^{-1}. The source of the frequency shift is unknown. Campbell & Roberts (1989) and Evans & Roberts (1990, 1991) predict that a horizontal magnetic field in the chromosphere would increase the frequencies of the f-modes by increasing the restoring force on the surface waves. The sign of the frequency shift may reverse at high wavenumber, however, in a more realistic model of the chromosphere with an appropriate magnetic field structure (Roberts 1991).

Duvall *et al.* (1991) report frequencies up to 6.7 mHz for p-modes in a lower wavenumber regime than we can explore with our data. Their measurements extend above the acoustic cutoff frequency of $\sim$ 5.3 mHz. At high wavenumber the acoustic cutoff frequency is approximately proportional to wavenumber (Gough 1990). Hence, our measured frequencies all lie below the acoustic cutoff. This is borne out by the measured 0° phase difference between velocity and intensity oscillations. This phase difference is indicative of standing waves (Deubner & Fleck 1989).

Two explanations have been put forward for the origin of the high frequency ridges observed by Duvall *et al.* (1991). Kumar *et al.* (1990) propose that waves are emitted isotropically from a source near the top of the convection zone. Waves traveling directly toward an overlying observed surface interfere with waves reflected from below to produce "mock modes." Balmforth & Gough (1990), on the other hand, propose a chromospheric cavity which couples to the familiar subphotospheric cavity to allow high frequency resonances.

The clear absence of chromospheric resonances in our data casts doubt on the existence of the chromospheric cavity required by the model of Balmforth & Gough. Either the reflection coefficient at the base of the corona is too low or the surface is too irregular to form a good cavity.

Acknowledgements

We would like to thank Douglas Gough and Bernard Roberts for interesting and illuminating discussions. D. N. F. is grateful to Tim Brown and Göran Scharmer for their suggestions concerning data analysis, to Paco Armas, Rolf Kevar, and Kermit Smith for their support at the Swedish Solar Observatory, and to Dick Shine at the Lockheed Palo Alto Research Laboratories for his consultation in software development. This work was funded by NASA contracts for SOUP (NAS 8-32805), OSL-CIP (NAS 5-26813), and SOI/MDI (NAS 5-30386), by NASA grant NGR-559, NSF grant ATM 90-22249, ONR grant N00014-89-J-1024, and by Lockheed Independent Research Funds.

References

[1] Balmforth, N. J., Gough, D. O., 1990, *Ap.J.*, **362**, 256–266

[2] Campbell, W. R., Roberts, B., 1989, *Ap.J.*, **338**, 538–556

[3] Chou, D.-Y., LaBonte, B. J., Braun, D. C., Duvall, T. L. Jr., 1991, *Ap.J.*, **372**, 314–320

[4] Deubner, F.-L., Fleck, B., 1989, *Astr. Ap.*, **224**, 245–252

[5] Duvall, T. L. Jr., Harvey, J. W., Jefferies, S. M., Pomerantz, M. A., 1991, *Ap.J.*, **373**.

[6] Evans, D. J., Roberts, B., 1990, *Ap.J.*, **356**, 704–719

[7] Evans, D. J., Roberts, B., 1991, *Ap.J.*, **371**, 387–395

[8] Gough, D. O., 1990, *Progress of Seismology of the Sun and Stars*, ed. Y. Osaki, H. Shibahashi, (Berlin: Springer), 283–318

[9] Hill, F., 1988, *Ap.J.*, **333**, 996–1013

[10] Kumar, P., Duvall, T. L. Jr., Harvey, J. W., Jefferies, S. J., Pomerantz, M. A., Thompson, M. J., 1990, *Progress of Seismology of the Sun and Stars*, ed. Y. Osaki, H. Shibahashi, (Berlin: Springer), 87–92

[11] Libbrecht, K. G., Woodard, M. F., Kaufman, J. M., 1990, *Ap. J. Suppl.*, **74**, 1129–1149.

[12] November, L. J., 1986, *Appl. Optics*, **25**, 392–397

[13] Roberts, B., 1991, private communication

[14] Schleicher, H., 1976, Dissertation, University of Göttingen

[15] Title, A. M., Tarbell, T. D., Wolfson, C. J., 1991, *Ap.J.*, in press

[16] Ulrich, R. K., Rhodes, E. J., 1977, *Ap.J.*, **218** 521–529

Figure 1: Scaled velocity-power spectrum. A portion of the collapsed power spectrum for the full field of view, with variable gray-scaling in the k and ν directions. Background has been subtracted. The noise visible at the top of the spectrum is an artifact of the scaling.

Figure 2: Background velocity power integrated over frequency. Background was fitted from the "quiet" subfield spectrum. Some correction has been made for the MTF of the telescope and seeing (see text).

Figure 3: Measured mode frequencies (from velocity spectra): ν vs. $\log_{10} k$. Frequencies of the f and p_1–p_6 ridges are plotted with 1 σ error bars. For $k < 3.96$ Mm^{-1}, frequencies were fitted from the full-field spectrum. At higher k the "quiet" subfield spectrum was used, as it had less noise.

Figure 4: Velocity power vs. mode frequency. Some correction has been made for the MTF of the telescope and seeing (see text).

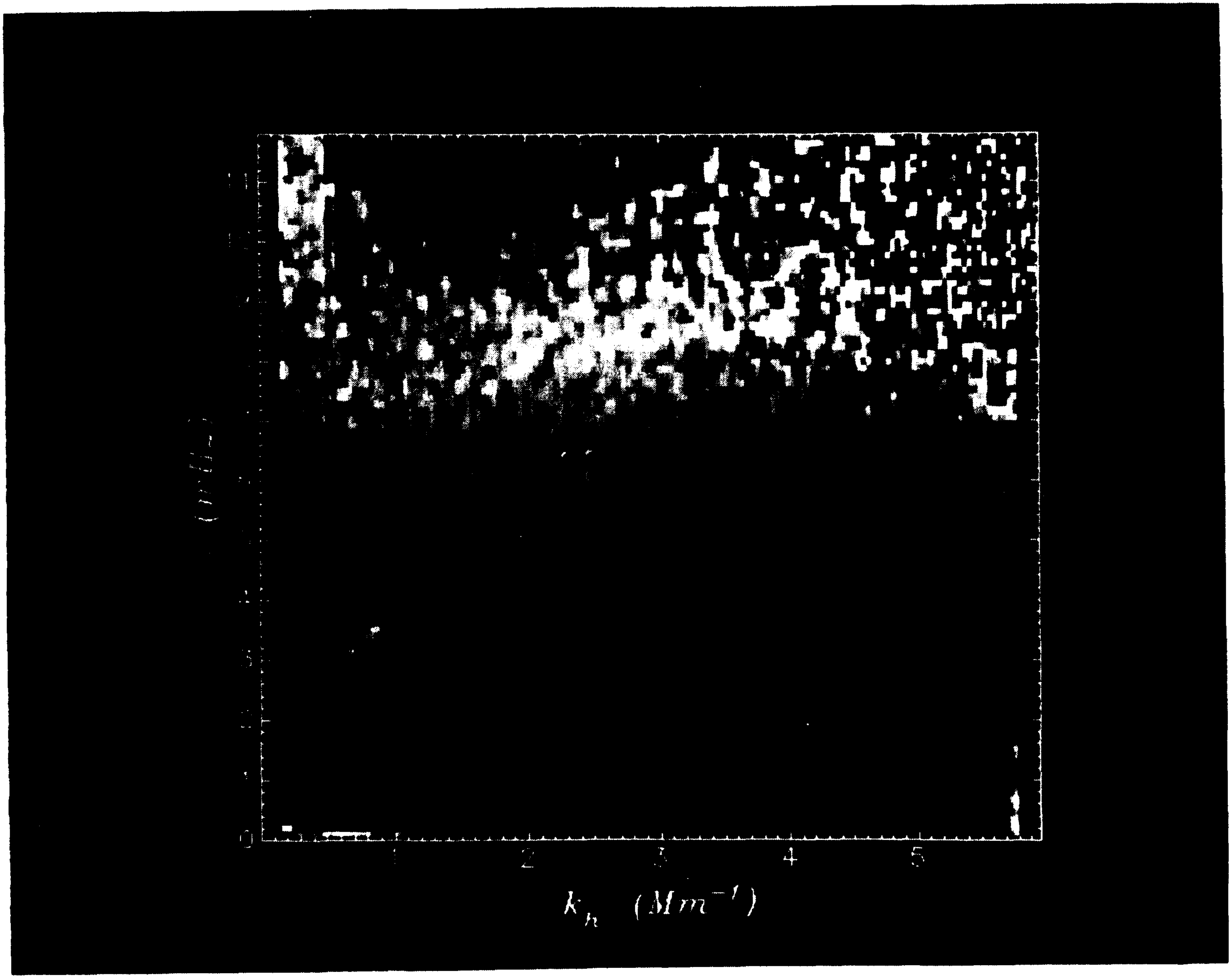

0
1
2
3
4
5
k_h (Mm^{-1})

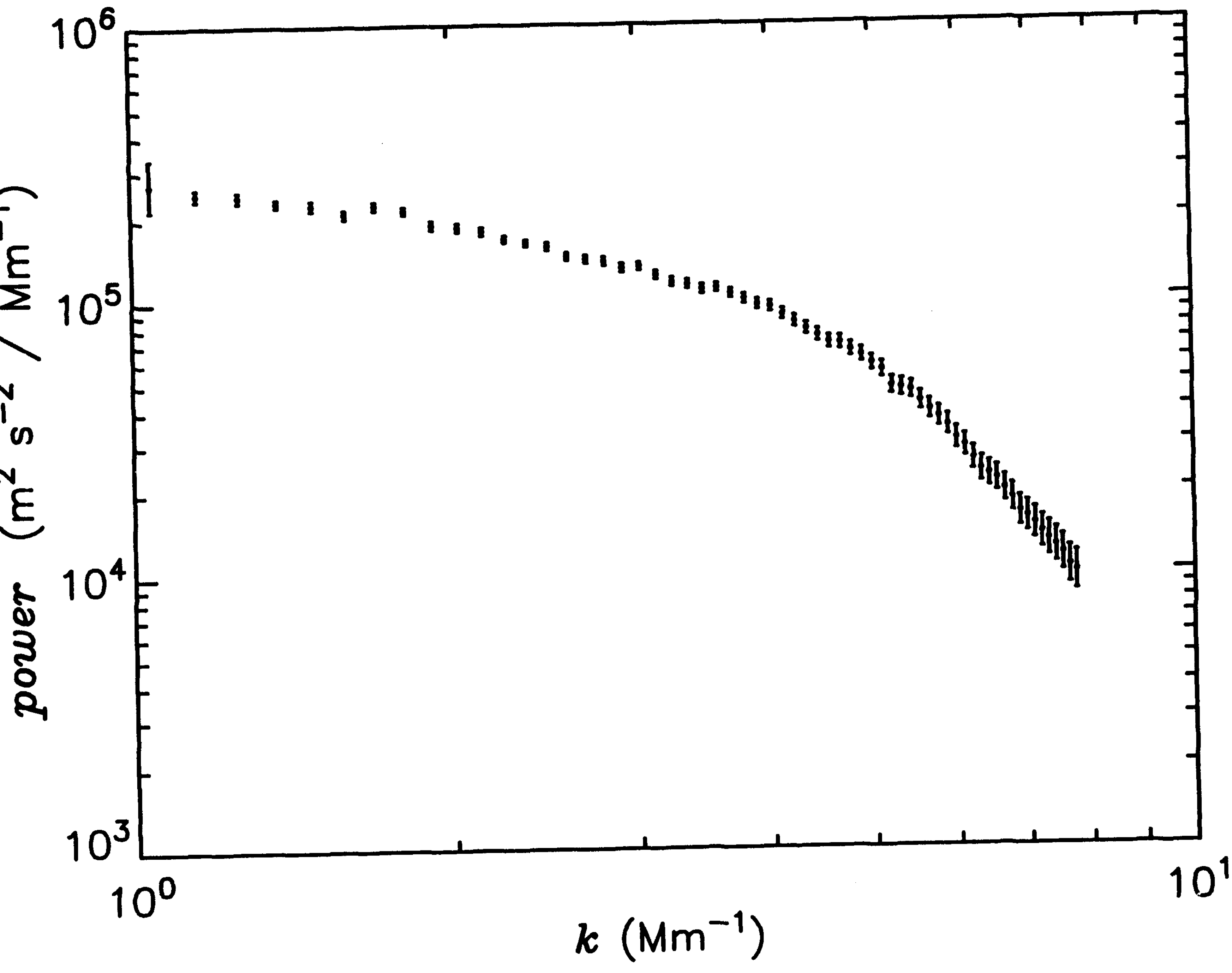

10^6
10^5
10^4
10^3
10^0
10^1
power (m^2 s^{-2} / Mm^{-1})
k (Mm^{-1})

Figure 2

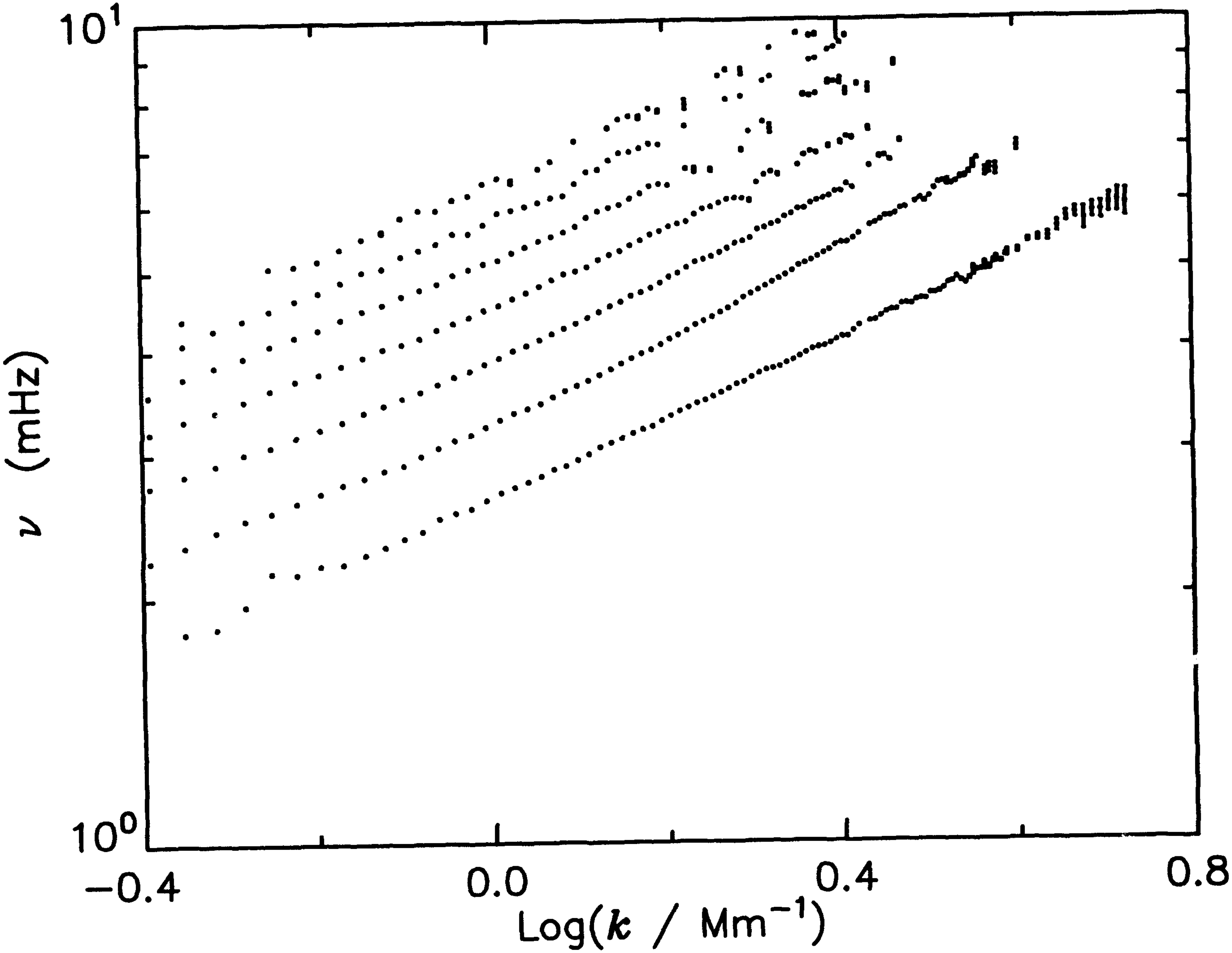

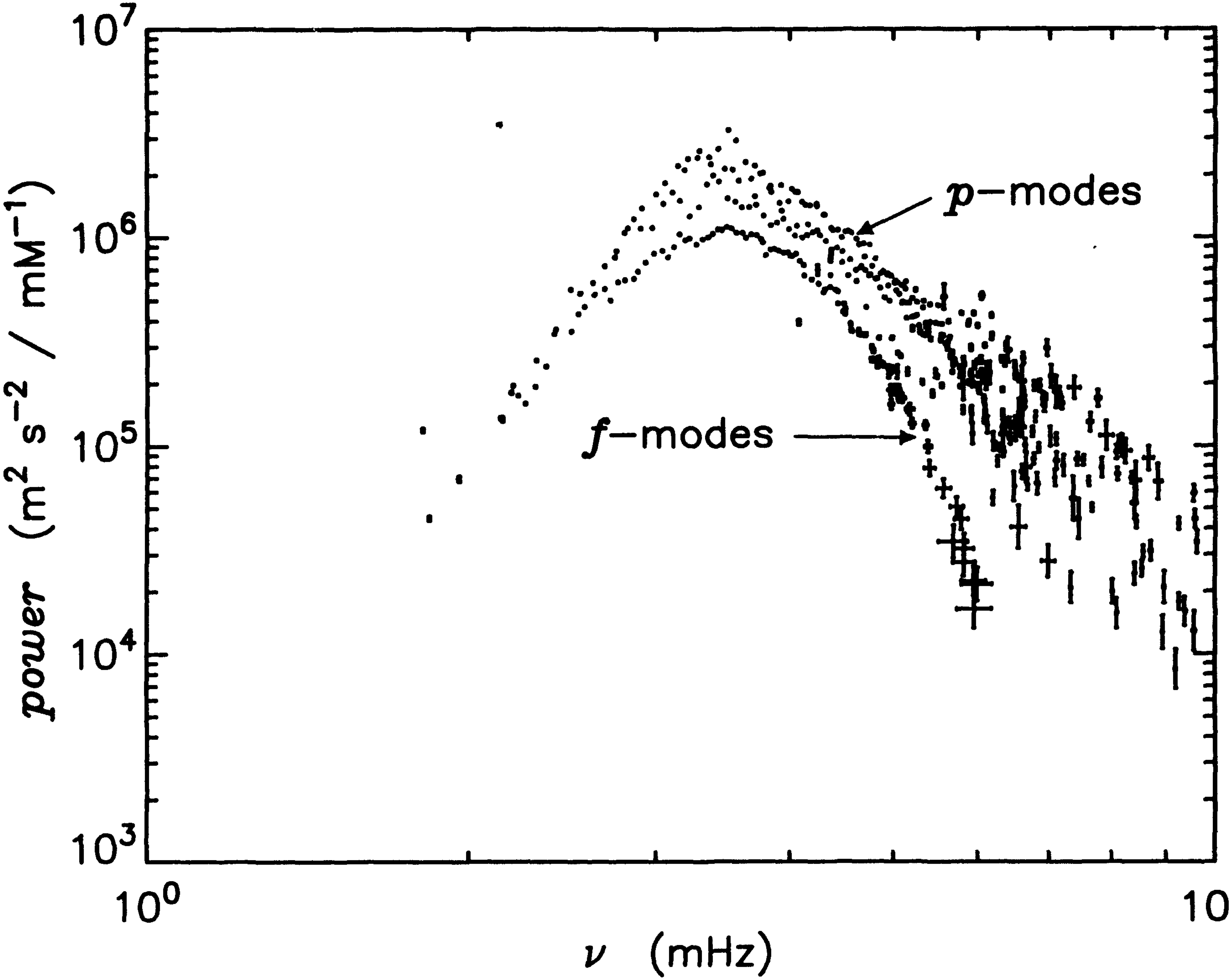

p–modes
f–modes
power (m^2 s^-2 / mM^-1)
ν (mHz)
10^7
10^6
10^5
10^4
10^3
10^0
10^1